

Backstepping control of a wind energy conversion systems based on a DFIG connected to the grid

Abstract. The backstepping control technique is a powerful nonlinear control method that has been successfully applied to various control problems in engineering. One of the areas where it has shown significant promise is in the control of the Doubly-Fed Induction Generator (DFIG), which is widely used in wind energy conversion systems; This study discusses the use of this method to control a nonlinear system presented as a doubly fed induction generator integrated into a wind power system connected to the grid. The nonlinear controller based on the backstepping technique is used in the rotor side converter (RSC), to control the electromagnetic torque and the reactive power, also, it is applied to control the power swapped with the grid and regulate the DC-bus voltage on the grid side converter (GSC). the backstepping control technique offers several advantages for controlling the DFIG in wind energy conversion systems. It provides robust and high-performance control, reduces torque ripple, and improves the overall efficiency of the system.

Streszczenie. Technika sterowania krokowego jest potężną nieliniową metodą sterowania, która została z powodzeniem zastosowana do różnych problemów sterowania w inżynierii. Jednym z obszarów, w których okazał się bardzo obiecujący, jest sterowanie podwójnie zasilanym generatorem indukcyjnym (DFIG), który jest szeroko stosowany w systemach konwersji energii wiatrowej; W pracy omówiono zastosowanie tej metody do sterowania nieliniowym układem przedstawionym jako dwustronnie zasilany generator indukcyjny zintegrowany z systemem energetyki wiatrowej podłączonym do sieci. Regulator nieliniowy oparty na technice backstepping jest stosowany w przekształtniku po stronie wirnika (RSC) do sterowania momentem elektromagnetycznym i mocą bierną, a także do sterowania mocą wymianianą z siecią oraz do regulacji napięcia szyny DC na konwerter po stronie sieci (GSC). technika sterowania krokowego ma kilka zalet przy sterowaniu DFIG w systemach konwersji energii wiatrowej. Zapewnia solidną i wydajną kontrolę, zmniejsza tętnienia momentu obrotowego i poprawia ogólną wydajność systemu. (Sterowanie wsteczne systemami konwersji energii wiatrowej w oparciu o DFIG podłączony do sieci)

Keywords: Wind turbine; DFIG; Backstepping; nonlinear control; Simulation; Modelling; Renewable energy.

Słowa kluczowe: Turbina wiatrowa; DFIG; Cofanie się; sterowanie nieliniowe; Symulacja; Modelowanie; Energia odnawialna.

Introduction

Wind energy is a form of solar energy [1]; it is one of the promising sources of renewable energy worldwide. It becomes more important with technological development. It's the process of converting wind energy into electricity. The kinetic energy of the wind is converted to mechanical power by the use of the wind turbines; in turn, the generators convert that mechanical power into electricity [2].

Doubly fed Induction Generators (DFIG) are becoming more current in industrial applications due to their high-power handling capability without increasing the power rating of the converters. It presents good performances of stability either in low-speed and in high-speed operation [3].

The DFIG is a highly nonlinear system that presents many difficulties to design a controlling system; this paper presents a theoretical context for a Backstepping control strategy; this technique is a new control method for nonlinear systems. It provides a recursive method for stabilizing the origin of a system and strict feedback form by choosing a Lyapunov function [4].

The backstepping technique is used in our study to achieve the following advantages over other control techniques:

Nonlinear Control: it is a nonlinear control technique, which makes it well-suited for controlling nonlinear systems like DFIGs. This allows for better performance and more accurate control of the system.

Decoupling the Rotor and Stator Currents: which is essential for efficient and stable operation of the machine. This allows the control system to achieve better control of both the rotor and stator currents, resulting in better performance and efficiency.

Robustness: Backstepping control is designed to be robust to disturbances and uncertainties in the system. This means that the control system can still perform well even if

there are variations in the wind speed or other environmental factors that affect the performance of the DFIG.

Smooth Control: Backstepping control provides smooth and continuous control of the DFIG. This is important for maintaining stable and efficient operation of the machine, as abrupt changes in the control signals can lead to instability and damage to the system.

Adaptability: it is an adaptable control technique that can be used for different types of DFIGs with different parameters and configurations. This allows the same control technique to be used across a range of DFIGs, reducing the need for customized control systems for each machine.

In the study made by M. DOUMI [5] the application of the Backstepping technique shows the Robustness, the reference tracking and the high performance of the controller.

In our study we attempt to integrate the DFIG with the tow backstepping based controllers to the grid, in order to show the advantages of the technique in real situations.

Modelling of the DFIG integrated with the wind power system

First, the mathematical model of the wind as well as the aerodynamic model of the turbine are presented, then the mechanical model of the wind turbine. Then for the transformation of mechanical energy into electrical energy, the operation of the DFIG will be briefly described, then it will be modelled

A. Wind model

The wind is the input energy vector of a wind chain, essential for calculating electricity production. Over time, the change in wind speed is modelled by an analytical function or generated by a statistical law from measurement data for a given site. In this study, the wind speed is

presented by a time variable function, modelled as a sum of some harmonics as shown in equation 1 [6].

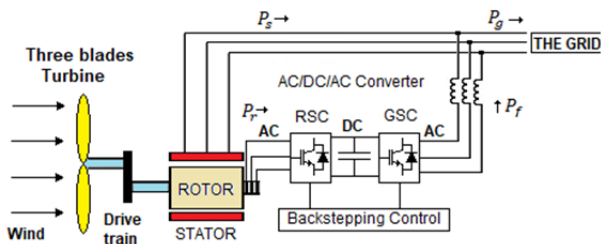


Fig. 1. Wind power conversion system

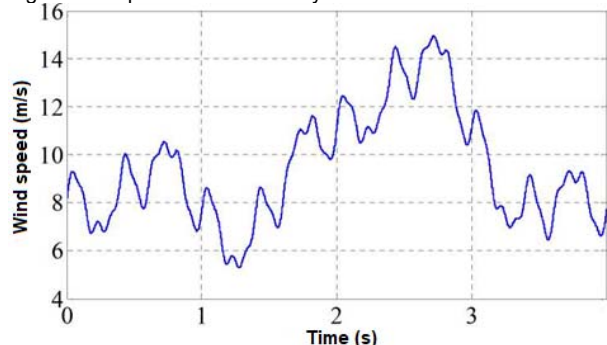


Fig. 2. Simulated profile of the wind speed

$$(1) \quad v(t) = 8.2 + 2 \sin(\omega t) - 1.75 \sin(3\omega t) + 1.5 \sin(5\omega t) - 1.25 \sin(10\omega t) + \sin(30\omega t) + 0.5 \sin(50\omega t) + 0.25 \sin(100\omega t)$$

Where: $\omega = 2\pi/10$

Figure 2 represents the simulated wind profile with an average speed of 8.2 [m/s].

B. Wind turbine modelling

The aerodynamic power of the turbine is expressed as a function of the power coefficient as [5]:

$$(2) \quad P_t = C_p P_v = \frac{1}{2} \rho \pi R^2 v^3 C_p(\beta, \lambda)$$

Where: $P_v = \frac{1}{2} \rho \pi R^2 v^3$ is the kinetic energy of the wind, and C_p is the power coefficient that represents the aerodynamic efficiency of the wind turbine that depends on its characteristic.

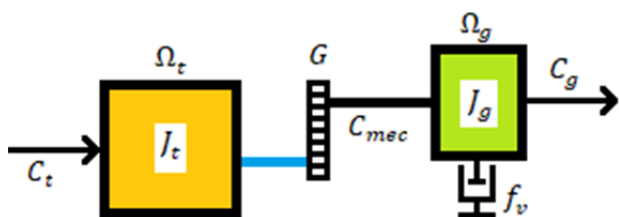


Fig. 3. Mechanical model of the wind turbine

The relative speed λ (tip speed ratio) is defined as the ratio between the linear speed of the blades ($R \cdot \Omega_t$) and the wind speed as follows:

$$(3) \quad \lambda = \frac{R \Omega_t}{v}$$

With: v is the wind speed (m/s).

ρ is the density of the air 1.225 (kg/m³) (at atmospheric pressure and 15 °C); R is the length of a blade (m); Ω_t is the mechanical speed of the turbine shaft (rad/s); β is the pitch angle.

The wind torque exerted on the turbine shaft can be obtained by dividing the aerodynamic power by the turbine's mechanical speed:

$$(4) \quad C_t = \frac{P_t}{\Omega_t} = \frac{1}{2\lambda} \rho \pi R^3 v^2 C_p(\beta, \lambda)$$

As C_p depends on the wind turbine's blades form, power, cite and pitch angle, this article uses the following expression as presented in equation 6 in order to proceed [6]:

$$(5) \quad C_p(\beta, \lambda) = 0.5 \left(\frac{116}{\lambda_i} - 0.4\beta - 5 \right) \exp\left(-\frac{21}{\lambda_i}\right) + 0.0068\lambda$$

$$\text{And } \frac{1}{\lambda_i} = \frac{1}{\lambda + 0.08\beta} - \frac{0.035}{\beta^3 + 1}$$

In order to adapt the slow speed of the turbine with the high speed of the generator, the multiplicator G is introduced as a gain, what gives:

$$(6) \quad C_g = \frac{C_t}{G}$$

$$(7) \quad \Omega_t = \frac{\Omega_g}{G}$$

From figure.3, the fundamental equation of the dynamics on the mechanical shaft of the generator can be expressed by:

$$(8) \quad J \frac{d\Omega_g}{dt} = C_{mec} = C_g - C_{em} - f_v \Omega_g$$

Where:

J is the total inertia of the system, formed by the inertia of the turbine J_t and the inertia of the generator J_g :

$$(9) \quad J = \frac{J_t}{G^2} + J_g$$

f_v : The viscous friction coefficient of the generator.

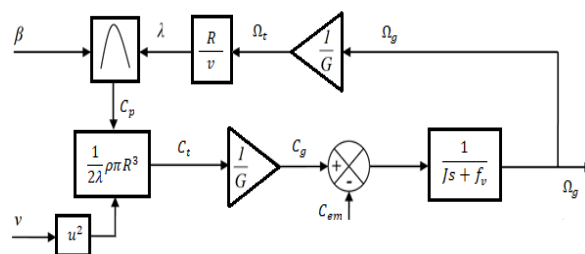


Fig. 4. Block diagram of the turbine model

C. Maximum power extraction

MPPT control without mechanical speed control is based on the assumption that wind speed varies very little in the steady-state, which implies that the acceleration torque of the turbine is considered to be zero [3].

$$(10) \quad J \frac{d\Omega_g}{dt} = C_{mec} = C_g - C_{em} - f_v \Omega_g = 0$$

If the effect of the torque due to viscous friction is neglected ($f_v \Omega_g = 0$), and β is considered constant, the wind speed and the electromagnetic torque reference can be estimated:

$$(11) \quad \hat{v} = \frac{\hat{\Omega}_t R}{\lambda_{opt}}$$

$$(12) \quad C_t^* = \frac{1}{2\lambda_{opt}^3} \rho \pi R^5 \hat{\Omega}_t^2 C_{p,max}$$

Where: \hat{a} : estimated value; and a^* : reference value.

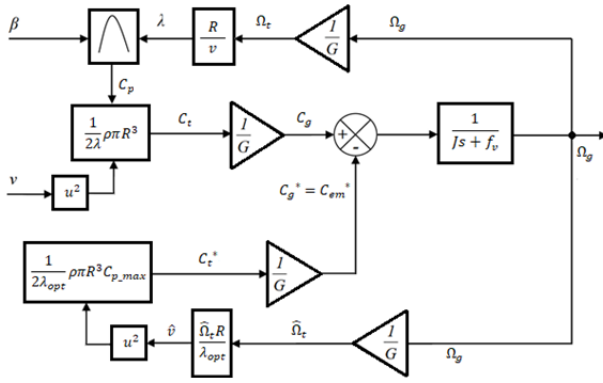


Fig. 5. MPPT block diagram without speed control

D. DFIG Modeling

The electrical model [7–10]

$$(13) \quad \begin{cases} v_{ds} = R_s i_{ds} + \frac{d}{dt} \Phi_{ds} - \omega_s \Phi_{qs} \\ v_{qs} = R_s i_{qs} + \frac{d}{dt} \Phi_{qs} + \omega_s \Phi_{ds} \end{cases}$$

$$(14) \quad \begin{cases} v_{dr} = R_r i_{dr} + \frac{d}{dt} \Phi_{dr} - \omega_{sr} \Phi_{qr} \\ v_{qr} = R_r i_{qr} + \frac{d}{dt} \Phi_{qr} + \omega_{sr} \Phi_{dr} \end{cases}$$

Stator and rotor fluxes

$$(15) \quad \begin{cases} \Phi_{ds} = L_s i_{ds} + L_m i_{dr} \\ \Phi_{qs} = L_s i_{qs} + L_m i_{qr} \end{cases}$$

$$(16) \quad \begin{cases} \Phi_{dr} = L_r i_{dr} + L_m i_{ds} \\ \Phi_{qr} = L_r i_{qr} + L_m i_{qs} \end{cases}$$

Active and reactive powers of the stator and rotor respectively:

$$(17) \quad \begin{cases} P_s = \frac{3}{2} (v_{ds} i_{ds} + v_{qs} i_{qs}) \\ Q_s = \frac{3}{2} (v_{qs} i_{ds} - v_{ds} i_{qs}) \end{cases}$$

$$(18) \quad \begin{cases} P_r = \frac{3}{2} (v_{dr} i_{dr} + v_{qr} i_{qr}) \\ Q_r = \frac{3}{2} (v_{qr} i_{dr} - v_{dr} i_{qr}) \end{cases}$$

The electromagnetic torque:

$$(19) \quad C_{em} = \frac{3}{2} p \frac{L_m}{L_s} (\Phi_{qs} i_{dr} - \Phi_{ds} i_{qr}) \quad (p: \text{the number of pairs of poles})$$

Often in the case of a medium and high power DFIG, the stator resistance R_s is neglected during the synthesis of its model under the assumption of orientation of the stator flux.

$$(20) \quad \begin{cases} v_{ds} = 0 \\ v_{qs} = \omega_s \Phi_{ds} \end{cases}$$

The active and reactive powers became:

$$(21) \quad \begin{cases} P_s = -\frac{3}{2} V_s \frac{L_m}{L_s} i_{qr} \\ Q_s = -\frac{3}{2} V_s \frac{L_m}{L_s} i_{dr} + \left(\frac{3V_s^2}{2L_s \omega_s} \right) \end{cases}$$

The electromagnetic torque:

$$(22) \quad C_{em} = -\frac{3}{2} p \frac{L_m}{L_s \omega_s} V_s i_{qr}$$

Thus, the equations of the relation between the rotor currents and voltages are establish:

$$(23) \quad \begin{cases} \dot{i}_{dr} = \frac{1}{\sigma L_r} (v_{dr} - R_r i_{dr} + g \sigma L_r \omega_r i_{qr}) \\ \dot{i}_{qr} = \frac{1}{\sigma L_r} (v_{qr} - R_r i_{qr} - g \sigma L_r \omega_r i_{dr} - \frac{g L_m}{L_s} V_s) \end{cases}$$

Backstepping Control

Backstepping is a method that breaks a complex nonlinear system into smaller single-input-single-output subsystems; each subsystem is considered a design step that provides a reference for the next one. This recursive design procedure connects the selection of a control Lyapunov function with the design of a feedback controller and ensures the system's global asymptotic stability [11–13].

A. Backstepping Control Of the RSC

1- Calculating the rotor reference currents

Defining the errors as the deferent between: the actual torque C_{em} and the reference torque C_{em}^* , the reactive stator power Q_s and its reference Q_s^* [14].

$$(24) \quad \begin{cases} Er_1 = C_{em}^* - C_{em} \\ Er_2 = Q_s^* - Q_s \end{cases}$$

Derivative of the equations 24, 22 and 21 gives:

$$(25) \quad \begin{cases} \dot{Er}_1 = \dot{C}_{em}^* + \frac{3}{2} p \frac{L_m}{L_s \omega_s} V_s \dot{i}_{qr} \\ \dot{Er}_2 = \dot{Q}_s^* + \frac{3}{2} V_s \frac{L_m}{L_s} \dot{i}_{dr} \end{cases}$$

The first Lyapunov function is chosen such as:

$$(26) \quad V_1 = \frac{1}{2} Er_1^2 + \frac{1}{2} Er_2^2$$

Its Derivative is:

$$(27) \quad \dot{V}_1 = \dot{Er}_1 Er_1 + \dot{Er}_2 Er_2$$

Replacing the equation 25 in 27

$$(28) \quad \begin{aligned} \dot{V}_1 = Er_1 \left(\dot{C}_{em}^* + \frac{3}{2} p \frac{L_m}{L_s \omega_s} V_s \frac{1}{\sigma L_r} \right. \\ \left. (v_{qr} - R_r i_{qr} - g \sigma L_r \omega_r i_{dr} - \frac{g L_m}{L_s} V_s) + \right. \\ \left. Er_2 \left(\dot{Q}_s^* + \frac{3}{2} V_s \frac{L_m}{L_s} \frac{1}{\sigma L_r} \right. \right. \\ \left. \left. (v_{dr} - R_r i_{dr} + g \sigma L_r \omega_r i_{qr}) \right) \right) \end{aligned}$$

$$\text{With: } \sigma = 1 - \frac{L_m^2}{L_s L_r}$$

In order to ensure that \dot{V}_1 is negative the following assumption is made:

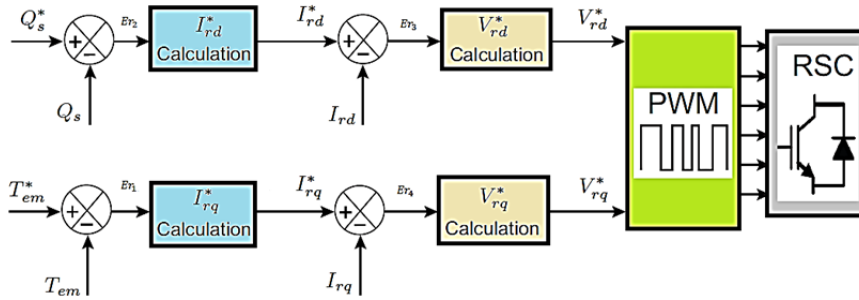


Fig. 6. RSC Backstepping control diagram

$$(29) \quad \begin{cases} -K_1 Er_1 = C_{em}^* + \frac{3}{2} p \frac{L_m}{L_s \omega_s} V_s \frac{1}{\sigma L_r} \\ \quad (v_{qr} - R_r i_{qr} - g \sigma L_r \omega_r i_{dr} - \frac{g L_m}{L_s} V_s) \\ -K_2 Er_2 = Q_s^* + \frac{3}{2} V_s \frac{L_m}{L_s \sigma L_r} \frac{1}{\sigma L_r} \\ \quad (v_{dr} - R_r i_{dr} + g \sigma L_r \omega_r i_{qr}) \end{cases}$$

Where K_1 and K_2 are positive constants. The derivative of the Lyapunov function becomes:

$$(30) \quad \dot{V}_1 = -K_1 Er_1^2 - K_2 Er_2^2 < 0$$

A, B and C are posed to simplify the equation

$$\begin{cases} A = \frac{p L_m}{2 L_s \omega_s \sigma L_r} \frac{3 V_s}{\sigma L_r} \\ B = g \sigma L_r \omega_r \\ C = \frac{3 V_s L_m}{2 L_s \sigma L_r} \end{cases}$$

The reference currents are chosen to achieve a stable functioning of the system, such as:

$$(31) \quad \begin{cases} i_{dr}^* = \frac{1}{C R_r} (K_2 Er_2 + Q_s^* + C v_{dr} + B C i_{qr}) \\ i_{qr}^* = \frac{1}{A R_r} (K_1 Er_1 + C_{em}^* + A v_{qr} - B A i_{dr} - A \frac{g L_m}{L_s} V_s) \end{cases}$$

2- Calculating the rotor reference Voltages

In this step, the rotor currents error is defined as follows:

$$(32) \quad \begin{cases} Er_3 = i_{dr}^* - i_{dr} \\ Er_4 = i_{qr}^* - i_{qr} \end{cases}$$

The derivative of this equation

$$(33) \quad \begin{cases} \dot{Er}_3 = i_{dr}^* - \frac{1}{\sigma L_r} (v_{dr} - R_r i_{dr} + g \sigma L_r \omega_r i_{qr}) \\ \dot{Er}_4 = i_{qr}^* - \frac{1}{\sigma L_r} (v_{qr} - R_r i_{qr} - g \sigma L_r \omega_r i_{dr} - \frac{g L_m}{L_s} V_s) \end{cases}$$

The second Lyapunov function used is

$$(34) \quad V_2 = \frac{1}{2} Er_3^2 + \frac{1}{2} Er_4^2$$

Where K_3 and K_4 are positive constants, and in order to ensure that \dot{V}_2 is negative:

$$(35) \quad \begin{cases} i_{dr}^* - \frac{1}{\sigma L_r} (v_{dr} - R_r i_{dr} + g \sigma L_r \omega_r i_{qr}) = -K_3 Er_3 \\ i_{qr}^* - \frac{1}{\sigma L_r} (v_{qr} - R_r i_{qr} - g \sigma L_r \omega_r i_{dr} - \frac{g L_m}{L_s} V_s) = -K_4 Er_4 \end{cases}$$

Therefore:

$$(36) \quad \begin{cases} v_{dr}^* = \sigma L_r \left(K_3 Er_3 + i_{dr}^* + \frac{R_r}{\sigma L_r} i_{dr} - g \omega_r i_{qr} \right) \\ v_{qr}^* = \sigma L_r \left(K_4 Er_4 + i_{qr}^* + \frac{R_r}{\sigma L_r} i_{qr} + g \omega_r i_{dr} + \frac{g L_m}{L_s} V_s \right) \end{cases}$$

B. Backstepping Control Of the GSC

The grid side converter is directly connected to the grid through an RL filter. Where the electrical currents are given by [15, 16]:

$$(37) \quad \begin{cases} \dot{i}_{fd} = -\frac{R_f}{L_f} \left(i_{fd} + \frac{1}{R_f} V_{fd} - \frac{\omega_s L_f}{R_f} i_{fq} \right) \\ \dot{i}_{fq} = -\frac{R_f}{L_f} \left(i_{fq} + \frac{1}{R_f} V_{fq} + \frac{\omega_s L_f}{R_f} i_{fd} - \frac{1}{R_f} V_{sq} \right) \end{cases}$$

The active and reactive powers are given in the oriented stator field by:

$$(38) \quad \begin{cases} P_f = V_{sq} i_{fq} \\ Q_f = -V_{sq} i_{fd} \end{cases}$$

The tracking error for the grid currents:

$$(39) \quad \begin{cases} Er_1 = i_{fd}^* - i_{fd} \\ Er_2 = i_{fq}^* - i_{fq} \end{cases}$$

The derivative:

$$(40) \quad \begin{cases} \dot{Er}_1 = i_{fd}^* + \frac{R_f}{L_f} \left(i_{fd} + \frac{1}{R_f} V_{fd} - \frac{\omega_s L_f}{R_f} i_{fq} \right) \\ \dot{Er}_2 = i_{fq}^* + \frac{R_f}{L_f} \left(i_{fq} + \frac{1}{R_f} V_{fq} + \frac{\omega_s L_f}{R_f} i_{fd} - \frac{1}{R_f} V_{sq} \right) \end{cases}$$

As the same procedure and calculation as for the RSC, the Lyapunov function choosing will be:

$$(41) \quad V = \frac{1}{2} Er_1^2 + \frac{1}{2} Er_2^2$$

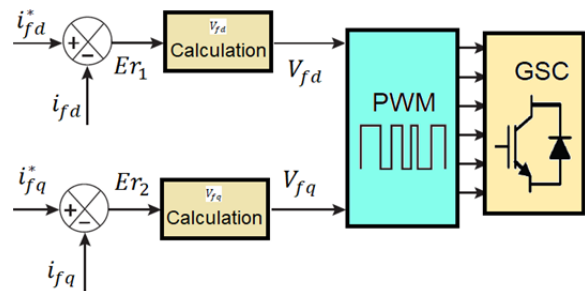


Fig. 7. GSC Backstepping control diagram

And in order to maintain it derivative negative:

$$(42) \quad \begin{cases} i_{fd}^* + \frac{R_f}{L_f} \left(i_{fd} + \frac{1}{R_f} V_{fd} - \frac{\omega_s L_f}{R_f} i_{fq} \right) = -K_1 Er_1 \\ i_{fq}^* + \frac{R_f}{L_f} \left(i_{fq} + \frac{1}{R_f} V_{fq} + \frac{\omega_s L_f}{R_f} i_{fd} - \frac{1}{R_f} V_{sq} \right) = -K_2 Er_2 \end{cases}$$

Therefore:

$$(43) \quad \begin{cases} V_{fd} = -L_f \left(\dot{i}_{fd}^* + \frac{R_f}{L_f} i_{fd} - \omega_s i_{fq} + K_1 E r_1 \right) \\ V_{fq} = -L_f \left(\dot{i}_{fq}^* + \frac{R_f}{L_f} i_{fq} + \omega_s i_{fd} - \frac{1}{L_f} V_{sq} + K_2 E r_2 \right) \end{cases}$$

Simulation and results

The simulations are done by utilizing the program MATLAB/Simulink. The DFIG and wind turbine parameters are as shown in the tables 1 and 2 respectively.

TABLE 1. DFIG Nominal Parameters

Parameter	Value
Power	1.5 MW
Stator Voltage	575 V
Nominal Frequency	50 Hz
Number of pole pairs (p)	2
Rotor resistor (Rr)	0.016 Ω
Rotor inductance (Lr)	0.16 H
Stator resistor (Rs)	0.023 Ω
Stator inductance (Ls)	0.18 H
Mutual inductance (Lm)	2.9 H

TABLE 2. Turbine Nominal Parameters

Parameter	Value
Power	1.5 MW
Optimal relative wind speed (λ_{opt})	9.9495
Cp max	0.5
Speed multiplier (G)	100
Inertia (J)	4.32 Kg.m ²
The viscous friction coefficient (fv)	1.5 N.m.s/rad

For the DC bus capacitor and the grid side RL filter the parameters are as presented in table 3.

TABLE 3. DC bus and RL filter parameters

Parameter	Value
C DC bus	10 mF
Rf	3 mΩ
Lf	0.3 H

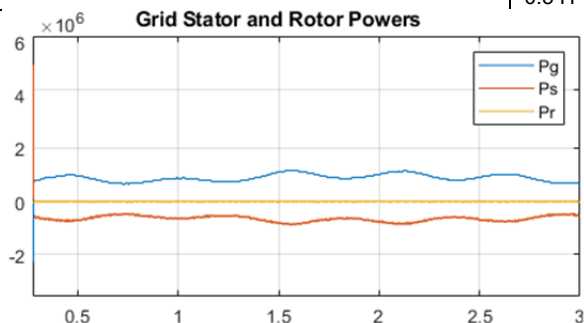


Fig. 8. Grid, Stator and rotor powers

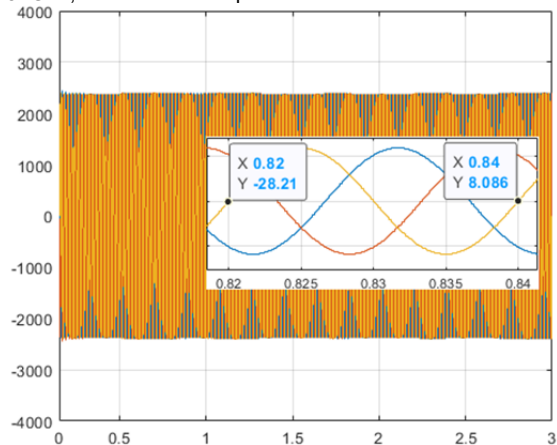


Fig. 9. The currents of the grid

The Fig.8 shows the three powers: The stator power P_s , the rotor power P_r passing through the filter assuming that $P_r = P_f$ (no losses), and the total power P_g . the grid power is the addition of all the powers.

As shown in Fig.9, the grid currents are sinusoidal with a frequency of: $f = 50$ Hz.

With the backstepping control in the RSC we were able to control the reactive power Q to its reference (0VAR), and the results are as in Fig.10.

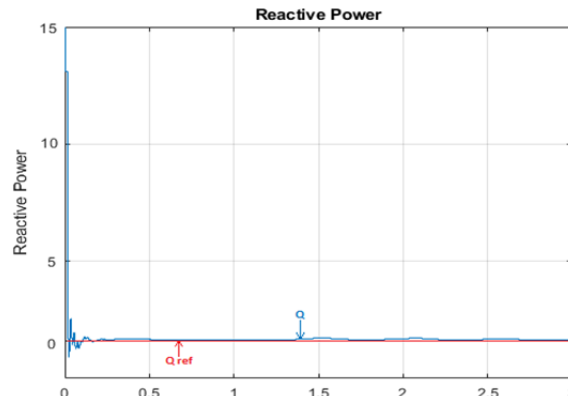


Fig. 10. The reactive power

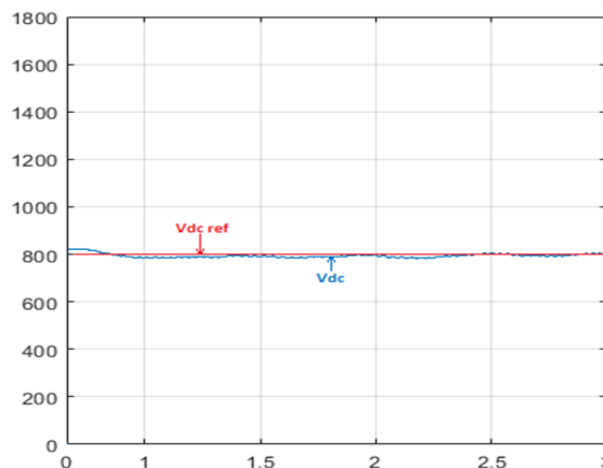


Fig. 11. DC bus voltage (DC-link)

The reference DC-link voltage is set to the value 800V. Fig.11 shows the DC voltage as it follows this reference.

Based on the obtained results (as shown in Fig. 10 and 11), we have achieved robustness and high performance with full reference tracking.

By connecting the generator to the electrical grid, we have provided a large amount of clean energy (as illustrated in Fig. 8), due to the controller's performance in extracting and tracking the maximum amount of wind energy.

Furthermore, backstepping control's recursive approach to designing a control law enables better tracking of the desired power output and improved regulation of the system's voltage and frequency (as depicted in Fig. 9), which are essential for maintaining a stable and reliable grid connection.

Conclusion

This paper proposes a nonlinear backstepping controller for wind energy conversion system based on DFIG. The Lyapunov approach shows the system's overall stability.

The suggested control method's is to provide high performance and better execution while making the system

insensitive to external disturbances and parametric fluctuations.

The backstepping control technique is particularly effective for DFIGs because it allows for the decoupling of the rotor and stator currents, which is necessary for efficient and stable operation of the machine. The technique also provides good performance in the presence of disturbances and uncertainties, which are common in renewable energy systems.

Further, two controllers are synthesized utilizing a classical PI and a backstepping controller to accomplish power reference tracking and parameter variation robustness. In ideal conditions, with no perturbations and no parameter fluctuations, the two controllers' tracking performances are comparable.

Overall, backstepping control is a powerful and effective control technique for DFIGs and is widely used in the renewable energy industry for controlling wind turbines and other renewable energy systems.

Authors:

Mr. Ghalem Abdelhak. Department of Electrotechnics, Faculty of Electrical Engineering, Interaction Networks-Converters-Machines Laboratory, E-mail: abdelhak.ghalem@univ-sba.dz

Prof. Naceri Abdellatif. Department of Electrotechnics, Faculty of Electrical Engineering, Interaction Networks-Converters-Machines Laboratory, E-mail: abdnaceri@yahoo.fr

Dr. Djeriri Youcef. Department of Electrotechnics, Faculty of Electrical Engineering, Intelligent Control and Electrical Power Systems Laboratory, E-mail: ydjeriri@yahoo.fr.

All: Djillali Liabes University of Sidi Bel Abbes 22000, Algeria.

REFERENCES

- [1] « How Do Wind Turbines Work? | Department of Energy ». <https://www.energy.gov/eere/wind/how-do-wind-turbines-work>.
- [2] « American Wind Energy Association ». http://www.awea.org/faq/wwt_basics.html.
- [3] E. A. Marouane, M. Hassane, et E. Chafik, « Backstepping control of a doubly fed induction generator integrated to wind power system », in 2nd International Conference on Electrical and Information Technologies, 2016, p. 1-6.
- [4] R. BOUSSAID et M. A. MORAD, « Commandes non linéaires d'une machine asynchrone double alimentation », Université Abou Bekr Belkaïd – Tlemcen, juin 20, 2016.
- [5] M'hamed DOUMI, Abdel Ghani AISSAOUI, Ahmed TAHOUR, Mohamed ABID, and Khalfallah TAHIR; Nonlinear Integral Backstepping Control of Wind Energy Conversion System Based on a Double-Fed Induction Generator; PRZEGLĄD ELEKTROTECHNICZNY, ISSN 0033-2097, R. 92 NR 3/2016
- [6] Y. Djeriri, « Commande directe du couple et des puissances d'une MADA associée à un système éolien par les techniques de l'intelligence artificielle », DJILLALI LIABES DE SIDI-BEL-ABBES, SIDI-BEL-ABBES, 2015. [En ligne]. Disponible sur: <https://www.researchgate.net/publication/295105086>
- [7] F. AZZEDDINE et M. M. MERZOUGA, « La commande par Backstepping de la MADA basée sur le principe de l'orientation du flux statorique », Université de M'sila, 2019.
- [8] O. BEN FEHIMA et H. ZROUG, « Commande par Backstepping d'une Génératrice Asynchrone à Double Alimentation (GADA) », UNIVERSITE MOHAMED BOUDIAF - M'SILA, 2020.
- [9] suman Ganesh kumar et sethi Suchit kumar, « Modelling of doubly fed induction generator connected with a wind turbine », Department of Electrical Engineering, National Institute of Technology Rourkela, 2014.
- [10] A. Rachid, Modélisation et Simulation des machines électriques. Ellipses, 2011.
- [11] A. Ahmad Taher et V. Sundarapandian, Backstepping Control of Nonlinear Dynamical Systems (Advances in Nonlinear Dynamics and Chaos (ANDC)). Elsevier Inc., 2021. [En ligne]. Disponible sur: <https://www.elsevier.com/books-and-journals>
- [12] K. Miroslav et S. Andrey, Boundary Control of PDEs. A Course on Backstepping Designs. U.S.A.: Society for Industrial and Applied Mathematics Philadelphia, 2008.
- [13] B. Wiktor et S. Jerzy, « SINGULARITY OF BACKSTEPPING CONTROL FOR NON-LINEAR SYSTEMS », in Proceedings of the American Control Conference, Anchorage, AK, mai 2002, p. 2689-2694.
- [14] D. M, A. A.G, T. A, A. M, et T. K, « Nonlinear Backstepping Control of a Double-Fed Induction Generator », in 4th International Conference on Renewable Energy Research and Application, Palermo, Italy, nov. 2015, p. 665-670.
- [15] Y. Djeriri, « Lyapunov-Based Robust Power Controllers for a Doubly Fed Induction Generator », Iranian Journal of Electrical and Electronic Engineering, Iran, p. 551-558, déc. 2020.
- [16] Abdelkader ACHAR, Youcef DJERIRI, Abderrahim BENTAALLAH, Salah HANAFI, Mohammed Abdeldjalil DJEHAF, Riyadh BOUDDOU; Lyapunov-Based Robust Power Controllers for a Wind Farm Using Parallel Multicell Converters; PRZEGLĄD ELEKTROTECHNICZNY, ISSN 0033-2097, R. 99 NR 4/2023